*Progress In Electromagnetics Research C, Vol. 33, 29–41, 2012*

# COMPACT HALF-MODE SUBSTRATE INTEGRATED WAVEGUIDE (HMSIW) FILTER WITH DUAL-MODE MICROSTRIP RESONATOR

**M. Zhou, M. X. Yu*, J. Xu, X. C. Zhang, and M. Y. Wang**

School of Physical Electronics, University of Electronic Science and Technology of China, Chengdu 610054, China

**Abstract**—A novel fourth-order half-mode substrate integrated waveguide (HMSIW) filter with dual-mode microstrip resonator is presented. The dual-mode resonator is etched on the top metal layer of HMSIW cavity, so the size can be reduced greatly. The filter has compact size and wide stopband in comparison with conventional SIW filters. Microstrip resonators and cavity resonators are integrated in one filter to achieve the goal of smaller size and better performance. Two filter samples are designed and fabricated, with good agreement between the measured and the simulated $S$-parameters.

## 1. INTRODUCTION

With the development of wireless and mobile communication systems, bandpass filters with better frequency selectivity and compact size have attracted much attention.

Microstrip dual-mode filters were proposed for applications in communication systems [1–5]. Each dual-mode resonator acts as two resonators, therefore, the size may be reduced in comparison with conventional microstrip resonator.

While focusing on the miniaturization of filters, increasing the $Q$-factor of filters should also be considered. Substrate integrated waveguide (SIW) filters have been studied extensively, which is due to their low loss, low cost and easy integration with other passive components. Some planar SIW filters with elliptic function have been reported in [6–16]. Each of them takes planar SIW cavities as resonators, so the sizes of filters are large in comparison with microstrip filters. HMSIW is a newly proposed planar guided wave

*Received 18 July 2012, Accepted 20 September 2012, Scheduled 27 September 2012*
* Corresponding author: Dr. Meng-xia Yu (yumengxia@263.net).

structure which keeps the advantages of SIW, but the size is nearly half reduced [17–19].

In this paper, we introduce a dual-mode resonator into HMSIW filters design to achieve compact size, which is etched on the top metal layer of HMSIW cavity. The electric response is examined by theory of coupling matrix. Two filter samples with compact sizes, better frequency selectivity and different transmission zero locations were fabricated and measured so as to validate the effectiveness of our proposed filters.

## 2. DESIGN OF THE FILTER

### 2.1. Dual-mode Resonator

The layout of a dual-mode resonator is shown in Fig. 1(a). The resonator comprises a $\lambda/2$ resonator and an open stub on its center plane. This symmetric structure can support two modes, i.e., an odd mode and an even mode. They can be calculated by function (1) and (2) [20], respectively. And equivalent layouts of odd and even mode are shown in Fig. 1(b). This resonator can use either its even mode or odd mode to couple an extra resonator. Its simple structure make it possible to integrate it with other kinds of resonators.

$$f_{\text{odd}} = \frac{(2n-1)\,c}{2L\sqrt{\varepsilon_{eff}}} \tag{1}$$

$$f_{\text{even}} = \frac{nc}{(L+2L_1)\sqrt{\varepsilon_{eff}}} \tag{2}$$

According to function (1) and (2), the resonant frequency of odd mode is determined by the length of the $\lambda/2$ resonator $L$ only, while

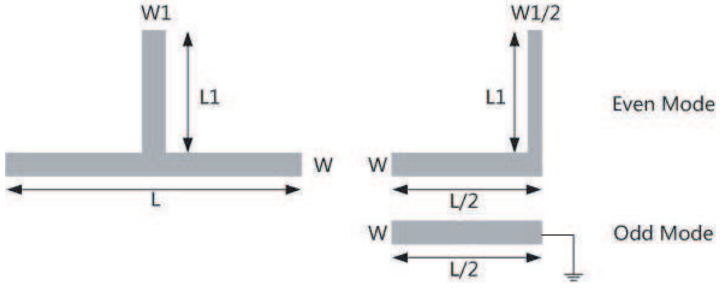

(a) (b)

**Figure 1.** Layout of (a) dual-mode resonator and (b) its equivalent odd- and even-mode, respectively.

the resonant frequency of even mode is determined by $L$ and the length of the open stub $L_1$ together. When this dual-mode resonator is utilized to construct a filter, the location of two transmission poles, odd-mode and even-mode, can be obtained by tuning $L$ and $L_1$ to proper length. If the resonant frequency of odd mode $f_{\text{odd}}$ is higher than the resonant frequency of even mode $f_{\text{even}}$, the transmission zero will be located in lower stopband, while the transmission zero will be located in higher stopband if $f_{\text{even}} > f_{\text{odd}}$. So we can move the location of the transmission zero by simply tuning the length of open stub $L_1$.

## 2.2. HMSIW Resonator

The layout of a conventional SIW and HMSIW resonators are shown in Fig. 2. The HMSIW resonator keeps the advantages of SIW resonator but the size is half reduced. The HMSIW resonator can be utilized to achieve the goal of more compact size with high $Q$-factor.

In this paper, a triangle HMSIW resonator is proposed to be integrated with dual-mode resonator mentioned above. Its layout is also shown in Fig. 2. And using 3-D electromagnetic simulation tool, the Ansoft HFSS, we can obtain the electric field distribution of this triangle HMSIW resonator's dominant mode as shown in Fig. 3.

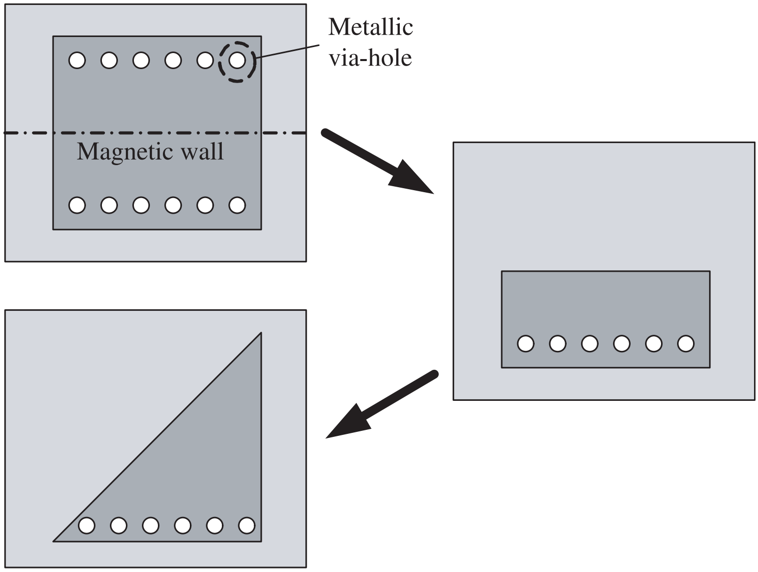


**Figure 2.** Layout of conventional SIW resonator, HMSIW resonator and triangle HMSIW resonator proposed in this paper, respectively.

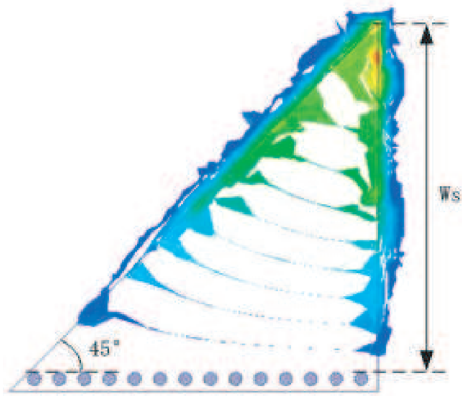


**Figure 3.** The electric field distribution of the dominant mode of triangle HMSIW resonator proposed.

Similar to conventional HMSIW resonator, the distance between the metallic via-hole and the open vertex of triangle, $W_s$, determines the resonant frequency of this resonator.

### 2.3. HMSIW Filter with Dual-mode Resonator

The top view and coupling scheme of the fourth-order with dual-mode resonator is shown in Figs. 4(a) and (b), respectively. The modes utilized here are all dominant modes.

As shown in Fig. 4, the corresponding coupling matrix $M$ can be written as [21]

$$M = \begin{bmatrix} 0 & M_{S1} & 0 & 0 & 0 & 0 \\ M_{S1} & M_{11} & M_{12} & M_{13} & 0 & 0 \\ 0 & M_{12} & M_{22} & 0 & M_{24} & 0 \\ 0 & M_{13} & 0 & M_{33} & M_{34} & 0 \\ 0 & 0 & M_{24} & M_{34} & M_{44} & M_{4L} \\ 0 & 0 & 0 & 0 & M_{4L} & 0 \end{bmatrix}$$

The nodal admittance matrix is given by [21]:

$$\{-j\,[G] + \Omega\,[W] + [M]\}\,[V] = [A]\,[V] = -j\,[I] \tag{3}$$

Here, [G] is a $(N+2)\times(N+2)$ matrix whose only nonzero entries are $G_{11} = G_{N+2,N+2} = 1$; $[M]$ is the coupling matrix; $[W]$ is a diagonal matrix of $(N+2)\times(N+2)$, with $W_{11} = W_{N+2,N+2} = 0$, and $W_{kk} = 1$.

The $S$-parameters are determined by

$$S_{11} = 1 + 2j \left[A^{-1}\right]_{1,1} \tag{4}$$

$$S_{21} = -2j \left[A^{-1}\right]_{N+2,1} \tag{5}$$

The electric field achieves maximum at the open ends of dual-mode resonator. However, the electric field of HMSIW cavity is minimized at the area under the open ends of dual-mode resonator. Therefore, the couplings HMSIW and dual-mode resonator is weak.

According to the coupling scheme, there will be one transmission zero. The situation with the transmission zero located in the higher stopband is considered first. Its corresponding coupling matrix $M$ is

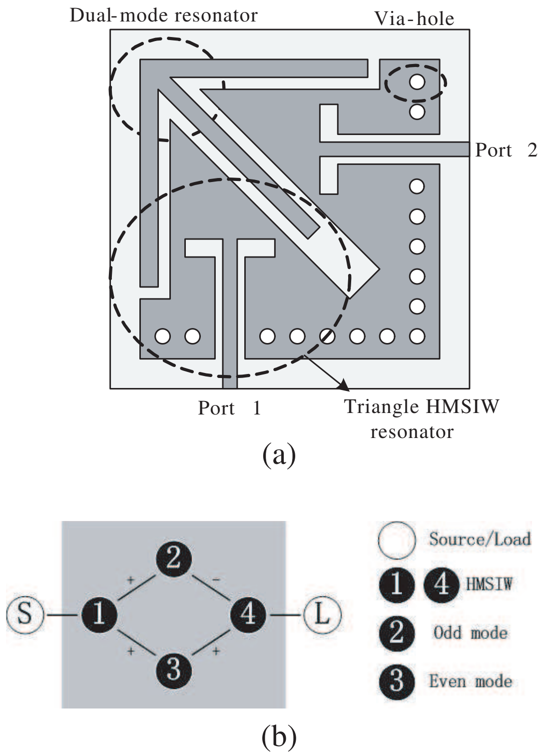


**Figure 4.** (a) Top view and (b) coupling scheme of the fourth-order filter with dual-mode resonator and two HMSIW resonators.

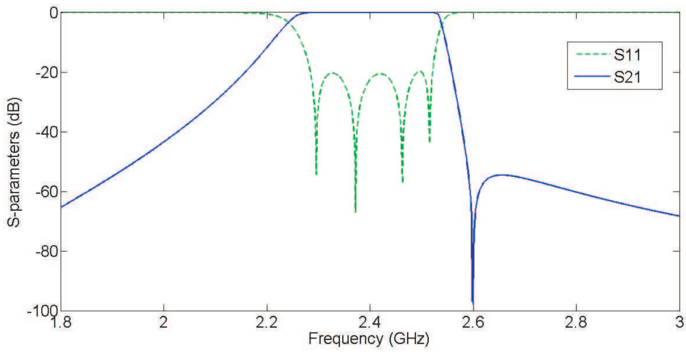


**Figure 5.** Synthesis frequency-dependent $S$-parameters for coupling matrix (transmission zero in higher stopband).

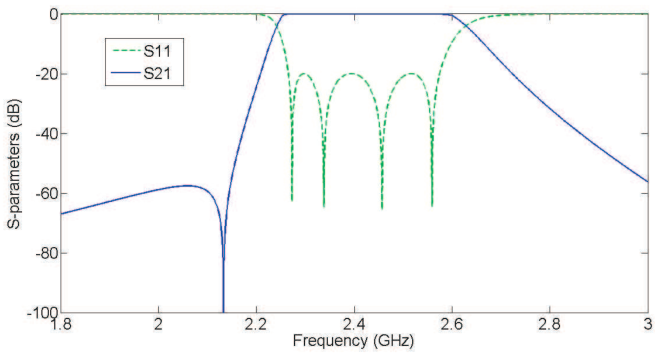


**Figure 6.** Synthesis frequency-dependent $S$-parameters for coupling matrix (transmission zero in lower stopband).

given by [21]

$$M = \begin{bmatrix} 0 & 1.0326 & 0 & 0 & 0 & 0 \\ 1.0326 & 0.0612 & 0.7928 & -0.4446 & 0 & 0 \\ 0 & 0.7928 & 0.4283 & 0 & 0.7928 & 0 \\ 0 & -0.4446 & 0 & -0.9199 & 0.4446 & 0 \\ 0 & 0 & 0.7928 & 0.4446 & 0.0612 & 1.0326 \\ 0 & 0 & 0 & 0 & 1.0326 & 0 \end{bmatrix}$$

Fig. 5 shows the synthesized $S$-parameters for coupling matrix $M$ with transmission zero in higher stopband.

Similarly, we can get the situation that the transmission zero is located in the lower stopband. Its corresponding coupling matrix $M$

is given by

$$M = \begin{bmatrix} 0 & 1.0336 & 0 & 0 & 0 & 0 \\ 1.0336 & -0.0465 & 0.7582 & 0.5019 & 0 & 0 \\ 0 & 0.7582 & -0.5006 & 0 & -0.7582 & 0 \\ 0 & 0.5019 & 0 & 0.8712 & 0.5019 & 0 \\ 0 & 0 & -0.7582 & 0.5019 & -0.0466 & 1.0336 \\ 0 & 0 & 0 & 0 & 1.0336 & 0 \end{bmatrix}$$

Fig. 6 shows the synthesized $S$-parameters for coupling matrix $M$ with transmission zero in lower stopband.

## 3. DESIGN AND RESULTS

The configuration of the filter is shown in Fig. 7. The resonant frequency of HMSIW resonators is mainly determined by $L_1$. $L_2$ and $L_c$ are used to control the resonant frequency of the dual-mode filter's odd mode and even mode, respectively. The location of the transmission zero can be controlled by tuning $L_c$. And as discussed in the dual-mode resonator part, the transmission zero will be moved from the higher stopband to lower stopband when $L_c$ is increased.

The simulated $S_{21}$-parameters of the filter with transmission located in different stopband for different values of $L_c$ are plotted in Fig. 8. As Fig. 8 shows, the transmission zero will move from higher stopband to lower stopband with $L_c$ is increased.

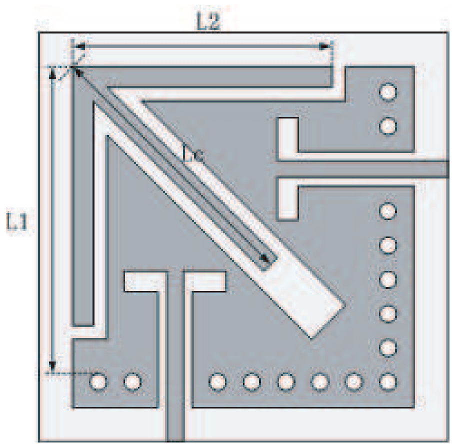


**Figure 7.** The configuration of the filter with dual-mode resonator.

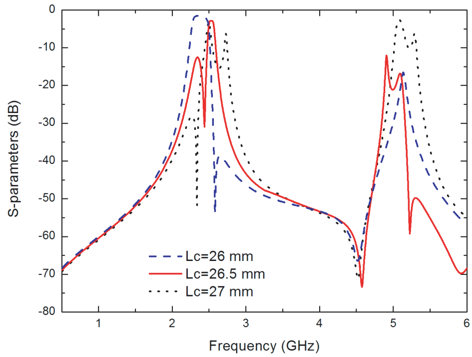


**Figure 8.** The simulated $S_{21}$-parameters for different values of $L_c$.

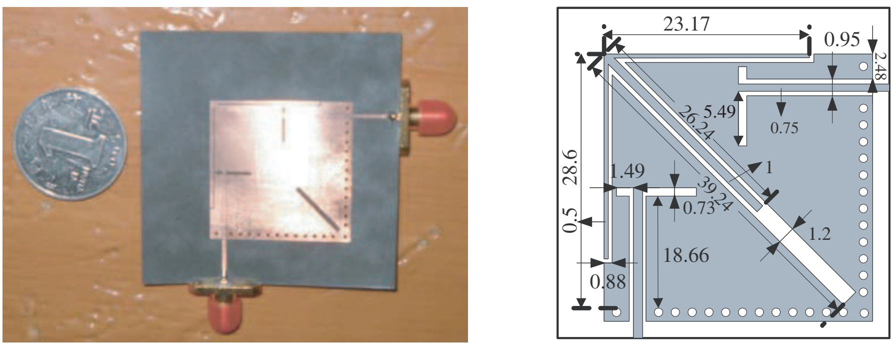


(a) (b)

**Figure 9.** The (a) photograph and (b) geometrical size of the fabricated filter A (transmission zero in higher stopband), respectively.

Two filter samples were fabricated on Rogers RT/duroid5880 with a substrate thickness of 0.254 mm and a dielectric constant of 2.2, with different transmission zero location.

Figures 9(a) and (b) show the photograph of the fabricated filter A with transmission zero located in higher stopband and its geometrical sizes, where the widths of the input and output 50 Ω microstrip lines are set to be 0.75 mm, respectively. The diameter of the via-holes is 1 mm.

The $S$-parameters of this filter are plotted in Fig. 10. The measured in-band return and insertion loss are below −14 dB and about 4 dB, respectively. The transmission zero is positioned at

2.6 GHz. And the second passband appears at 5 GHz, which is about 2.08 times of the center frequency. As shown in Fig. 10, frequency with the out-band suppression below −50 dB ranges from the transmission zero to about 4.8 GHz, which is 2 times of the center frequency. And the parasitic passband shown in Fig. 10 is produced by the high mode of dual-mode resonator.

By mainly tuning the length of the dual-mode resonator, we can move the location of the transmission zero to the lower stopband. Figs. 11(a) and (b) show the photograph of the fabricated filter B with transmission zero located in higher stopband and its geometrical

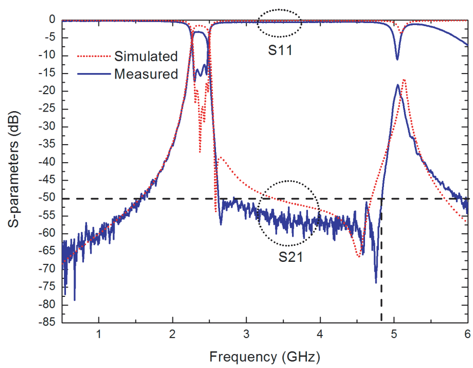


**Figure 10.** Frequency-dependent $S$-parameters of the fabricated filter A (transmission zero in higher stopband).

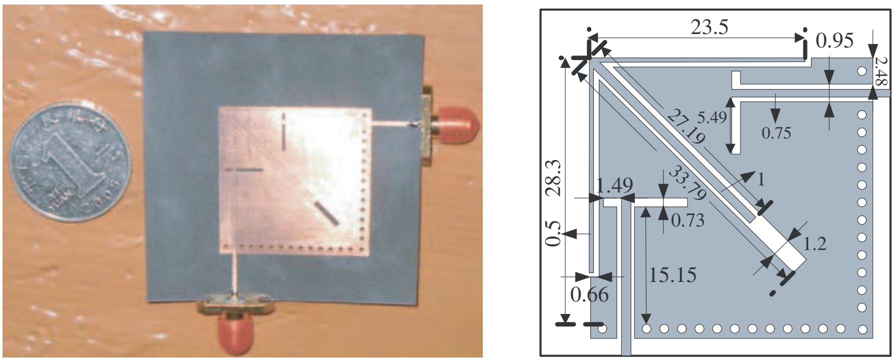


(a) (b)

**Figure 11.** The (a) photograph and (b) geometrical size of the fabricated filter B (transmission zero in lower stopband), respectively.

**Table 1.** Comparison with the reported filters.

| Ref. | Type | Size ( $\lambda g \times \lambda g$ ) | $f_0$ (GHz) | 3 dB FBW | IL/RL (dB) | $\frac{\Delta f_{3\,dB}}{\Delta f_{20\,dB}}$ | $\lvert S_{21} \rvert$ (dB) |
|---|---|---|---|---|---|---|---|
| [5] | Microstrip Filter | 0.42 × 0.36 | 2.4 | 7% | 2.7/15 | 0.486 | > 30 (2.75–4.25 GHz) |
| [16] | SIW Filter | 0.69 × 0.69 | 3.4 | 12% | 1.6/18 | 0.444 | > 30 (3.75–7.5 GHz) |
| [19] | HMSIW Filter | 1.59 × 0.33 | 7.25 | 7% | 1.7/12.5 | 0.278 | > 20 (8 – 11 GHz) |
| This work | Filter A | 0.32 × 0.32 | 2.4 | 8% | 4/14 | 0.511 | > 50 (2.58–4.8 GHz) |
| | Filter B | 0.32 × 0.32 | 2.4 | 8% | 2.5/10 | 0.503 | > 30 (2.75–4.3 GHz) |

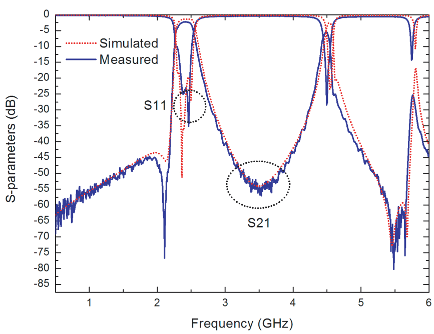


**Figure 12.** Frequency-dependent $S$-parameters of the fabricated filter B (transmission zero in lower stopband).

sizes, where the widths of the input and output $50\,\Omega$ microstrip lines are set to be 0.75 mm, respectively. The diameter of the via-holes is 1 mm.

The $S$-parameters of this filter are plotted in Fig. 12. The measured insertion and return losses are 2.5 dB and below $-10$ dB. The transmission zero is located at 2.1 GHz. The slight shift of center frequency is mainly attributed to the fabricated tolerance.

The proposed filters with microstrip dual-mode resonator are compact in comparison with conventional SIW filters. Since HMSIW resonators and microstrip resonator are integrated in one filter, the filters presented in this paper have high $Q$-factor and good out-band suppression. And the filters have better frequency selectivity.

Table 1 is the comparison among the proposed filters and reported ones. The ratio of $\Delta f_{3\,\mathrm{dB}}$ to $\Delta f_{20\,\mathrm{dB}}$ is 0.511 and 0.503, which show good passband selectivity. The proposed filters have the advantage of compact size and good out-band suppression.

## 4. CONCLUSION

In this paper, a compact HMSIW filter with dual-mode resonator is presented, which is etched on the top metal layer of HMSIW cavity. The filter has better frequency selectivity and wide stopband in comparison with conventional SIW filters. Two filter samples were fabricated. Good filter performance is achieved as demonstrated by our simulated as well as measured $S$-parameters.

## ACKNOWLEDGMENT

This work is supported by the Fundamental Research Funds for the Central Universities (ZYGX2010J046).

## REFERENCES

1. Zhu, L. and K. Wu, "A joint field/circuit model of line-to-ring coupling structures and its application to the design of microstrip dual-mode filters and ring resonator circuits," *IEEE Transactions Microwave Theory & Techniques*, Vol. 47, No. 10, 1938–1948, 1999.
2. Lee, J. R., J. H. Cho, and S. W. Yun, "New compact bandpass filter using microstrip 1/4 resonators with open stub inverter," *IEEE Microwave Guide Wave Letters*, Vol. 10, No. 12, 526–527, 2000.
3. Wei, C. L., B. F. Jia, Z. J. Zhu, and M. Tang, "Design of different selectivity dual-mode filters with e-shaped resonator," *Progress In Electromagnetics Research*, Vol. 116, 517–532, 2011.
4. Tyurnev, V. V. and A. M. Serzhantov, "Dual-mode split microstrip resonator for compact narrowband bandpass filters," *Progress In Electromagnetics Research C*, Vol. 23, 151–160, 2011.
5. Liao, C. K., P. L. Chi, and C. Y. Chang, "Microstrip realization of generalized Chebyshev filters with box-like coupling schemes," *IEEE Transactions Microwave Theory & Techniques*, Vol. 55, No. 1, 147–153, 2007.
6. Zhang, X. C., Z. Y. Yu, and J. Xu, "Novel band-pass substrate integrated waveguide (SIW) filter based on complementary split

ring resonators (SCRRs)," *Progress In Electromagnetics Research*, Vol. 72, 39–46, 2007.

7. Hao, Z. C., W. Hong, X. P. Chen, J. X. Chen, K. Wu, and T. J. Cui, "Multilayered substrate integrated waveguide (MSIW) elliptic filter," *IEEE Microwave and Wireless Components Letters*, Vol. 15, No. 2, 95–97, 2005.
8. Shen, T. M., C. F. Chen, T. Y. Huang, and R. B. Wu, "Design of vertically stacked waveguide filters in LTCC," *IEEE Transactions Microwave Theory* & *Techniques*, Vol. 55, No. 8, 1771–1779, 2007.
9. Chen, B. J., T. M. Shen, and R. B. Wu, "Dual-band vertically stacked laminated waveguide filter design in LTCC technology," *IEEE Transactions Microwave Theory* & *Techniques*, Vol. 57, No. 6, 1554–1562, 2009.
10. Shen, W., L. S. Wu, X. W. Sun, W. Y. Yin, and J. F. Mao, "Novel substrate integrated waveguide filters with mixed cross coupling (MCC)," *IEEE Microwave and Wireless Components Letters*, Vol. 19, No. 11, 701–703, 2009.
11. Ismail, A., M. S. Razalli, M. A. Mahdi, R. S. A. Raja Abdullah, N. K. Noordin, and M. F. A Rasid, "X-band trisection substrate-integrated waveguide quasi-elliptic filter," *Progress In Electromagnetics Research*, Vol. 85, 133–145, 2008.
12. Wang, R., L. S. Wu, and X. L. Zhou, "Compact folded substrate integrated waveguide cavities and bandpass filter," *Progress In Electromagnetics Research*, Vol. 84, 135–147, 2008.
13. Zhang, Z. G., Y. Fan, Y. J. Cheng, and Y.-H. Zhang, "A novel multilayer dual-mode substrate integrated waveguide complementary filter with circular and elliptic cavities (SICC and SIEC)," *Progress In Electromagnetics Research*, Vol. 127, 173–188, 2012.
14. Zhang, Z. G., Y. Fan, Y. J. Cheng, and Y.-H. Zhang, "A compact multilayer dual-mode substrate integrated circular cavity (sicc) filter for x-band application," *Progress In Electromagnetics Research*, Vol. 122, 453–465, 2012.
15. Chen, L. N., Y. C. Jiao, Z. Zhang, and F.-S. Zhang, "Miniaturized substrate integrated waveguide dual-mode filters loaded by a series of cross-slot structures," *Progress In Electromagnetics Research C*, Vol. 29, 29–39, 2012.
16. Shen, W., W. Y. Yin, X. W. Sun, and J. F. Mao, "Compact substrate integrated waveguide (SIW)transversal filter with triple-mode microstrip resonator," *Asia-Pacific Microwave Conference Proceedings (APMC)*, 1875–1878, 2010.

17. Hong, W., Y. Wang, Q. H. Lai, and B. Liu, "Half mode substrate integrated waveguide: A new guided wave structure for microwave and millimeter wave application," *Joint 31st International Conference Infrared Millimeter Waves and 14th International Conference on Terahertz Electronics*, 219, Shanghai, China, 2006.
18. Liu, B., W. Hong, Y. Q. Wang, Q. H. Lai, and K. Wu, "Half mode substrate integrated waveguide (HMSIW) 3 dB coupler," *IEEE Microwave and Wireless Components Letters*, Vol. 17, No. 1, 22–24, 2007.
19. Zhang, X. C., J. Xu, Z. Y. Yu, and Y. L. Dong, "C-band half mode substrate integrated waveguide (HMSIW) filter," *Microwave and Optical Technology Letters*, Vol. 50, No. 2, 275–277, 2008.
20. Zhang, X. Y., J. X. Chen, Q. Yue, and S. M. Li, "Dual-band bandpass filters using stub-loaded resonators," *IEEE Microwave and Wireless Components Letters*, Vol. 17, No. 8, 583–585, 2007.
21. Amari, S., U. Rosenberg, and J. Bornemann, "Adaptive synthesis and design of resonator filters with source/load-multiresonator coupling," *IEEE Transactions Microwave Theory & Techniques*, Vol. 50, No. 8, 1969–1978, 2002.